88684.docx

SIRT1 ameliorates acute liver failure by reducing ferroptosis and pyroptosis via the p53/GPX4/GSDMD axis

Xing-Nian Zhou, Quan Zhang, Hong Peng, Yu-Jie Qin, Yu-Hong Liu, Lu Wang, Ming-Liang Cheng, Xin-Hua Luo, Hong Li

Abstract

Background: Acute liver failure (ALF) has a high mortality with widespread hepatocyte death involving ferroptosis and pyroptosis. The silent information regulator sirtuin 1(SIRT1)-mediated deacetylation affects multiple biological processes, including cellular senescence, apoptosis, sugar and lipid metabolism, oxidative stress, and inflammation.

Aim: To investigate the association between ferroptosis and pyroptosis and the upstream regulatory mechanisms.

Methods: This study included 30 patients with ALF and 30 healthy individuals who underwent serum alanine aminotransferase (ALT) and aspartate aminotransferase (AST) testing. C57BL/6 mice were also intraperitoneally pretreated with SIRT1, p53, or GPX4 inducers and inhibitors and injected with lipopolysaccharide (LPS)/ D-galactosamine (D-GalN) to induce ALF. GSDMD-/- mice were used as an experimental group. Histological changes in liver tissue were monitored by hematoxylin and eosin staining. ALT, AST, glutathione, reactive oxygen species, and iron levels were measured using commercial kits. Ferroptosis- and pyroptosis-related proteins were detected by western blotting and quantitative real-time polymerase chain reaction. SIRT1, p53, and GSDMD were assessed by immunofluorescence analysis.

Results: Serum AST and ALT levels were elevated in patients with ALF. SIRT1, SLC7A11, and GPX4 protein expression was decreased and acetylated p53 (Ac-p53), p53, GSDMD, and ACSL4 protein levels were elevated in human ALF liver tissue. In the p53 and ferroptosis inhibitor-treated and GSDMD^{-/-} groups, serum IL-1β, TNF-α, IL-6, IL-2 and CCL2 levels were decreased and hepatic impairment was mitigated. In mice with GSDMD knockout, p53 was reduced, GPX4 was increased, and ferroptotic

events (depletion of SLC7A11, elevation of ACSL4, and iron accumulation) were detected. *In vitro*, knockdown of p53 and overexpression of GPX4 reduced AST and ALT levels, the cytostatic rate, and GSDMD expression, restoring SLC7A11 depletion. Moreover, an SIRT1 agonist and overexpression alleviated acute liver injury and decreased iron deposition compared with results in the model group, accompanied by reduced p53, GSDMD, and ACSL4, and increased SLC7A11 and GPX4. Inactivation of SIRT1 exacerbated ferroptotic and pyroptotic cell death and aggravated liver injury in LPS/D-GalN-induced *in vitro* and *in vivo* models.

Conclusion: SIRT1 activation attenuates LPS/D-GalN-induced ferroptosis and pyroptosis by inhibiting the p53/GPX4/GSDMD signaling pathway in ALF.

Keywords: SIRT1; Ferroptosis; Pyroptosis; p53/ Glutathione peroxidase 4

CORE TIP

/Gasdermin D; Acute liver failure

In our study, we investigated the involvement of ferroptosis and pyroptosis in ALF using LPS/D-GalN-induced ALF model mice. Our results showed that SIRT1 activation alleviated ALF through p53/GPX4/GSDMD, which mediated the ferroptosis and pyroptosis crosstalk. Our study established a link between ferroptosis and pyroptosis and the upstream regulatory mechanisms. These results may lead to the identification of potential therapeutic targets for ALF.

INTRODUCTION

Acute liver failure (ALF) is a rare and severe consequence of abrupt hepatocyte injury, with a mortality rate of up to 30%^[1]. ALF is caused by various factors, including drugs, toxins, virus, and metabolic diseases. The central event in ALF is the excessive and uncontrolled mass death of hepatocytes through necrosis and apoptosis, which can cause DNA damage and oxidation stress, accompanied by an inflammatory storm^[2, 3]. Accumulating evidence has suggested that ferroptosis and pyroptosis, which are novel programed modes of cell death that are distinct from necrosis, apoptosis, and autophagy, play critical roles in ALF by each mediating different

immunological effects and inflammatory responses^[4-6].

Ferroptosis is characterized by intracellular iron overload, decreased glutathione peroxidase 4 (GPX4) activity, and accumulation of lipid reactive oxygen species (ROS)^[7]. SLC7A11, a component of the system XC⁻ antiporter located in the cell membrane, is involved in glutathione (GSH) synthesis ^[8]. Le et al^[9] showed that transcriptional suppression of SLC7A11 by p53 resulted in inhibited cystine uptake and sensitized cells to ferroptosis. p53 plays a critical role in the cellular response to various stresses, including DNA damage, hypoxia, nutrition starvation, and oncogene activation^[10]. Additionally, p53 promotes ferroptosis by inhibiting cystine metabolism and ROS activity ^[9,11].

Pyroptosis is a lytic cell death induced by pathogen infection or an endogenous challenge [12]. When cells receive internal and external danger signals, pattern recognition receptors initiate various inflammasomes to activate caspase 1, leading to cleavage of the pyroptosis executor gasdermin D (GSDMD) into the active N terminal and inactive C terminal. The active N terminal fragment translocates from the cytosol into the medial cell membrane, forming a large number of sieve membrane pores, resulting in the release of cell contents, including IL-1β and IL-18, into the extracellular space. Recruitment of immune cells for targeted migration to the injury site mediates secondary immune damage^[13]. Our previous study showed that GSDMD-mediated pyroptosis of hepatocytes played an important role in the pathogenesis of ALF [14]. Furthermore, GSDMD knockout reduced hepatocyte death and inflammatory responses, thus alleviating ALF. However, the relationship between ferroptosis and pyroptosis in ALF is unknown.

SIRT1, which is an NAD+-dependent protein deacetylase, regulates the acetylation of specific transcription factors and proteins, including p53. SIRT1 is involved in various functions, such as energy metabolism, stress responses, inflammation, and redox homeostasis^[15, 16]. Deacetylation of p53 by SIRT1 may act as a protective shield in sepsis-induced liver injury ^[17].

In our study, we investigated the involvement of ferroptosis and pyroptosis in ALF using LPS/D-GalN-induced ALF model mice. Our study established an association

between ferroptosis and pyroptosis and the upstream regulatory mechanisms. These results may lead to the identification of potential therapeutic targets for ALF.

MATERIALS AND METHODS

Patients

Samples from 30 patients with ALF and 30 healthy individuals were collected from the Affiliated Hospital of Guizhou Medical University. ALF was diagnosed by following the definition in the 2017 EASL Acute Liver Failure Guidelines^[18]. Whole livers of seven patients with ALF and donor trimmed portions from three liver transplant recipients were collected. This study was approved by the Ethics Committee of the Affiliated Hospital of Guizhou Medical University (2018 Lun Audit No. 036) and complied with the ethical guidelines of the 1975 Declaration of Helsinki. The tissue donors and/or their families provided informed consent for the use of human residual material for research purposes.

Mouse model and drug treatment

Male C57BL/6 mice (8–10 weeks, 22–26 g) were purchased from SPF Biotechnology Co. (Beijing, China). Male GSDMD systemic knockout (GSDMD-/-) mice (C57BL/6J strain, 6–8 weeks) were a generous gift from Shao Feng's Laboratory, Beijing Institute of Life Sciences, China. Laboratory animal production license No. SYXK (Guizhou) 2023-0002, and laboratory animal use license No. SYXK (Guizhou) 2023-0002. All animals were kept in the Laboratory Animal Centre of Guizhou Medical University. The animal experimental methods designed in this study were reviewed and approved by the Animal Ethics Committee of Guizhou Medical University. The mice were maintained in a 12-h light-dark cycle environment and had free access to water and food. The mice acclimated to the environment for 1 week before the experiments.

The mice were randomly divided into the nine following experimental groups (n=10 per group): vehicle (phosphate-buffered saline), resveratrol (a SIRT1 activator; MedChemExpress, New Jersey, United States; 30 mg/kg, intraperitoneal injection [i.p.] for 14 days), EX527 (a SIRT1 inhibitor; Sigma, St. Louis, Missouri, USA; 5

mg/kg, i.p. for 14 days), pifithrin-α (a p53 inhibitor; MedChemExpress; 2.2 mg/kg, i.p. for 3 days), nutlin-3α (a p53 inducer; MedChemExpress; 12 mg/kg, i.p. for 7 days), liproxstatin-1 (a ferroptosis inhibitor; MedChemExpress; 10 mg/kg, i.p. for 14 days), RSL3 (a ferroptosis inducer, Sigma, 2 mg/kg, i.p. for 7 days), GSDMD^{-/-}, and ALF model. The mice were pre-treated as described above before establishing the model.

To establish the ALF model, all groups except for the vehicle group, were injected with lipopolysaccharide (LPS) (Sigma, $10 \mu g/kg$, i.p.) and D-GalN (Sigma, 300 mg/kg, i.p.). After 48 h, survival was recorded and the surviving mice were sacrificed. Blood was collected from the eyeball vein and centrifuged at $3000 \times g/\min$ for 15 min. The serum was separated and stored at -80° C. Liver tissues were harvested by portal vein perfusion. Some of the specimens were fixed using paraformaldehyde for 48 h, and a pathological examination was performed. The remaining tissues were quickly stored at -80° C.

Iron assay

Liver tissues and cells were homogenized in an ice bath using the Iron Assay Kit (BC4355; Solarbio, Beijing, China). The samples were centrifuged at $4000 \times g$ at 4° C and the supernatant was removed. The supernatants were added to a 96-well plate, and the absorbance was measured at 520 nm with a microplate reader.

Hematoxylin and eosin staining

Liver tissues were fixed in 4% paraformaldehyde for 24 h and dehydrated by a concentration gradient of ethanol solutions, followed by paraffin embedding. Tissue sections were cut, de-waxed, rehydrated, and stained with hematoxylin and eosin (H&E). The sections were subjected to microscope analysis.

Immunofluorescence analysis

Liver tissues were collected and routinely embedded in optimal cutting tissue. The sections were dewaxed three times for 30 min each and dehydrated three times for 30 min each, followed by three washes with phosphate-buffered saline. Liver sections were stained with antibodies against SIRT1 (ab110304; Abcam), p53 (80077-1-RR; Proteintech), and GSDMD (ab219800; Abcam) overnight at 4°C. After extensive

washing, the sections were incubated with the respective fluorescent secondary antibodies (ab150115, ab150077; Abcam) for 2 h at room temperature.

Short interfering RNA transfection

SIRT1, p53, GPX4, and negative control (NC) short interfering (siRNAs) were obtained from GeneChem (China). HL7702 cells were transfected with siRNAs using Lipofectamine 3000 (Invitrogen, USA) by following the manufacturer's instructions. After 6 h, the culture medium was replaced with fresh complete medium and the cells were cultured for 48 h.

Alanine aminotransferase and aspartate aminotransferase assays

The levels of alanine aminotransferase (ALT) and aspartate aminotransferase (AST) in serum were assessed using the ALT Kit (E-BC-K235-M; Elabscience, China) and AST Kit (E-BC-K236-M; Elabscience, China) by following the manufacturers' instructions.

ROS assay

ROS activity in cells was measured by a fluorescent probe (DCFH-DA) (Beyotime, Shanghai, China). HL7702 cells in a six-well plate were treated with D-GalN/LPS (D-GalN 15 mmol/L+LPS 100 μ g/mL) for 24 h, and DCFH-DA (2 μ L/well) was added for 30 min at 37°C. The cells were washed three times with serum-free medium. DCFH-DA was measured by flow cytometric analysis.

Quantitative real-time polymerase chain reaction

Liver tissue was lysed by Trizol (Omega, USA). Total RNA was extracted and tested for concentration and purity. The RNA was reverse transcribed using a reverse transcription kit (Takara, Japan) and cDNA was synthesized. Expression levels of mRNA were evaluated using the SYBR Green detection system (Takara, Japan). All samples were measured in triplicate and gene expression was normalized with GAPDH mRNA levels. The primer sequences were as follows: glyceraldehyde 3-phosphate dehydrogenase (GAPDH), (forward) AGGTCGGTGTGAACGGATTTG and (reverse) GGGGTCGTTGATGGCAACA; p53, (forward) CCCCTGCATCTT TTGTCCCT and (reverse) AGCTGGCAGAATAGCTTATTGAG; GPX4, (forward) TGTGCATC CCGCGATGATT and (reverse) CCCTGTACTTATCCAGGCAGA;

GSDMD, (forward) ATGCC ATCGGCCTTTGAGAAA and (reverse)

AGGCTGTCCACCGGAATGA; SLC7A11, (forward)

GGCACCGTCATCGGATCAG and (reverse) CTCCACAGGCAGACCAGAAAA; and acyl-CoA synthetase long-chain family member 4 (ACSL4)., (forward) CCTGAGGGGCTTGAAATTCAC and (reverse) GTTTCGGTGTGAACGGATTTG.

Western blotting

Liver tissues and cells were rinsed twice with phosphate-buffered saline buffer and lysed on ice with RIPA lysis solution (Solarbio). The protein samples were separated on 10% sodium dodecyl sulfate-polyacrylamide gels and transferred to polyvinylidene fluoride membranes (Millipore, USA). The membranes were incubated with mouse anti-Sirt1 (1:1000; Abcam; ab110304), mouse anti-p53 (1:1000; Abcam; ab26), rabbit anti-p53 (acetyl K382) (1:1000; Abcam; ab75754), mouse anti-GPX4 (1:2000; Proteintech; 67763-1-Ig), rabbit anti-GSDMD (1:1000; Abcam; ab129800), rabbit anti-SLC7A11 (1:2000; Origene; TA351958), and rabbit anti-ACSL4 (1:2000; Origene; TA349566) overnight at 4°C. The membranes were incubated with secondary anti-mouse HRP-conjugated antibodies (1:5000; Proteintech; SA00001-1) or secondary anti-rabbit Horseradish Peroxidase-conjugated antibodies (1:5000; Proteintech; SA00001-2) for 2 h at room temperature. The signals were visualized using enhanced chemiluminescence reagent (CLiNX; Chemiscop, Shanghai, China).

Statistical analysis

Statistical analysis was conducted using Prism 8.3.0 (GraphPad, USA). Values are expressed as the mean \pm standard of at least three independent experiments. The normality and the homogeneity of variance were checked by the Shapiro–Wilk test before Student's t-test and one-way analysis of variance analysis. Student's t-test was used to compare data between two groups, while one-way analysis of variance analysis was used for comparison between multiple groups. Statistical significance was considered if P was <0.05.

RESULTS

Ferroptosis and pyroptosis are triggered in liver tissue in patients with ALF

To examine the potential role of ferroptosis and pyroptosis in ALF, we first examined

the inflammatory status, liver function biomarkers, and markers for ferroptosis and pyroptosis in the serum samples from patients with ALF. We found that AST, ALT, and inflammatory factor levels were increased in human ALF serum (Figure 1A). Iron staining showed iron accumulation in liver tissue in patients with ALF (Figure 1B-C). Additionally, the ferroptotic markers GPX4 and SLC7A11 showed decreased protein expression, whereas p53 and ACSL4 proteins, which are positive regulators of ferroptosis, were elevated in human ALF liver tissue (Figure 1D). In line with previous studies [14], GSDMD, which is a key regulatory factor of pyroptosis, was increased in human ALF tissue (Figure 1E). We also found that p53 and Ac-p53 were elevated and SIRT1 was decreased in human ALF tissue (Figure 1F).

FIGURE 1 Ferroptosis and pyroptosis occurred in human ALF. (A) The levels of AST, ALT, TNF-α, IL-1β and IL-6 were changed in serum samples of 30 normal patients and serum samples of ALF (n=30 in every group). $^aP < 0.05$, $^bP < 0.01$. (B) iron staining (Scale bar:100μm and 33.3μm) of normal liver tissue and ALF. a : normal liver tissue (Scale bar:100μm), b: ALF liver tissue(Scale bar:100μm), c: normal liver tissue (Scale bar:33.3μm), d: ALF liver tissue(Scale bar:33.3μm). (C) Iron detection of normal liver tissue and ALF. $^bP < 0.01$. (D) Western blot analyses of GPX4, SLC7A11, p53 and ACSL4 proteins were performed in normal patients and ALF. Data were presented as the mean ± SD of 3 independent experiments. $^aP < 0.05$, $^bP < 0.01$. (E) Western blot analyzed GSDMD protein (n=3), $^bP < 0.01$. (F) Western blot showed SIRT1 and Ac-p53 proteins in normal patients and ALF (n=3). $^aP < 0.05$, $^bP < 0.01$.

Inhibition of p53/GPX4/GSDMD-mediated ferroptosis and the pyroptosis pathway protects mice against LPS/D-GalN-induced ALF

We observed an induction of ferroptosis and pyroptosis in human ALF liver tissues, accompanied by increased p53 protein expression. To further examine the mechanism of ferroptosis and pyroptosis in ALF, we inhibited ferroptosis and pyroptosis in mice with ALF induced by LPS/D-GalN. Untreated mice were first pretreated with pifithrin-α and liproxstatin-1, which inhibits GPX4 consumption^[19, 20]. GSDMD^{-/-}

mice were used as another experimental group. H&E staining of liver sections showed that mice pre-treated with pifithrin-α or liproxstatin-1 and GSDMD^{-/-} mice had less structural damage in liver tissue, and most liver lobules were structurally intact compared with those in the ALF model group. These mice also showed a prolonged survival compared with those in the ALF model group (Figure 2A, B). Furthermore, mice pre-treated with pifithrin-α or liproxstatin-1 and GSDMD^{-/-} mice showed a reduction in elevated serum levels of IL-1β, TNF-α, IL-6, IL-2, and CCL2, which are inflammatory factors associated with pyroptosis, compared with those in the ALF model group (Figure 2C). Western blotting and quantitative real-time polymerase chain reaction (PCR) showed that mice with pre-treatment with pifithrin-α and liproxstatin-1 had reduced protein and mRNA levels of GSDMD and ferroptotic markers (ACSL4 and p53) compared with those in the ALF model group. We also found that GSDMD imice showed increased GPX4 and SLC7A11 and decreased p53 and ACSL4, accompanied by a decrease in iron accumulation (Figure 2D-G). Notably, p53 protein levels were markedly lower in GSDMD^{-/-} mice than in ALF mice, but they were not affected by liproxstatin-1. However, p53 mRNA levels in the liproxstatin-1 group were downregulated (Figure 2D). An immunofluorescence assay showed a decrease in GSDMD expression in the groups treated with pifithrin- α and liproxstatin-1 (Figure S1A).

To gain insight into the potential mechanisms of ferroptosis and pyroptosis in ALF induced by LPS/D-GalN, HL7702 cells transfected with p53 siRNAs targeting p53 and plasmid overexpressing GPX4 were stimulated with LPS/D-GalN for 24 h. We then detected the cellular AST and ALT contents. We found that LPS/D-GalN significantly increased AST and ALT, while knocking down p53 and overexpressing GPX4 reduced AST and ALT (Figure 3A, B). We further examined iron, ROS, GSH, and lipid peroxidation products, and found that knocking down p53 and overexpressing GPX4 significantly reduced GSH, malondialdehyde (MDA), and ROS contents compared with those in the AFL model group (Figure 3C–E). Western blotting and quantitative real-time PCR showed that when p53 was knocked down and GPX4 was overexpressed, SLC7A11 protein and mRNA expression levels were

restored compared with control levels. This change occurred at the same time as a decrease in ACSL4 expression (Figure 3F-H). Notably, GSDMD expression was also reduced in the sh-p53 group compared with the sh-NC group. To evaluate the relationships between p53, GPX4, and GSDMD, we overexpressed GPX4 in HL7702 cells, and found that AST and ALT levels were increased (Figure S1A). Furthermore, with GPX4 overexpression, iron, ROS, and GSH contents and ferroptotic events were higher than those in the control group (Figure S1A). Western blotting and quantitative real-time PCR showed that SLC7A11 protein and mRNA levels were downregulated, while p53, ACSL4, and GSDMD protein and mRNA levels were upregulated in the GPX4 knockdown group compared with the sh-NC group (Figure S2B-C). GPX4 and GSDMD play a prominent role in the occurrence of ferroptosis and pyroptosis. p53 promotes ferroptosis by inhibiting cystine metabolism and ROS activity. However, the relationships between p53, GPX4, and GSDMD are unknown. These results showed that the suppression of ferroptosis and pyroptosis attenuated LPS/D-GalN-induced hepatocyte injury by inhibiting the p53/GPX4/GSDMD signaling pathway and lipid peroxidation.

FIGURE 2 Inhibition of the p53/GPX4/GSDMD signaling pathway attenuates ALF in vivo. (A) Macroscopic examinations of mouse livers were collected, and liver sections were stained with H&E ($100\times$). a: normal group general image, b: model group general image, c: p53 inhibitor group general image, d: ferroptosis inhibitor group general image, e: GSDMD^{-/-} group general image, f: normal group microscope image, g: model group microscope image, h: p53 inhibitor group microscope image, i: ferroptosis inhibitor group microscope image, j: GSDMD^{-/-} group microscope image. (B) The administration of pifithrin- α , liproxstatin-1 and GSDMD knock out improved the median survival in mice treated with D-GalN/LPS. (C) Multi-factor kit for the detection of IL-1 β , TNF- α , IL-6, IL-2 and CCL2 in mouse serum. Data were presented as the mean \pm SD of 5 independent experiments. ${}^{a}P < 0.05$, ${}^{b}P < 0.01$. (D) Western blot analyses of p53, GPX4, SLC7A11, ACSL4 and GSDMD proteins were performed (n = 3 in every group). Data were presented as the mean \pm SD of 3

independent experiments. ${}^{a}P < 0.05$, ${}^{b}P < 0.01$. (E) Western blot analyses of GSDMD protein were performed (n = 3 in every group). Data were presented as the mean \pm SD of 3 independent experiments. ${}^{a}P < 0.05$, ${}^{b}P < 0.01$. (F) Iron Kit for Iron Detection. Data were presented as the mean \pm SD of 5 independent experiments. ${}^{a}P < 0.05$, ${}^{b}P < 0.01$. (G) qRT-PCR analyses of p53, GPX4, SLC7A11, ACSL4 and GSDMD proteins were performed (n = 3 in every group). Data were presented as the mean \pm SD of 3 independent experiments. ${}^{a}P < 0.05$, ${}^{b}P < 0.01$.

FIGURE 3 Inhibition of the p53/GPX4/GSDMD signaling pathway exacerbated acute liver injury in vitro. (A-B) The levels of ALT and AST were changed in serum samples of HL7702 cells (n=3). ${}^{a}P < 0.05$, ${}^{b}P < 0.01$. (C-E) The levels of Iron, ROS and GSH were changed in serum samples of HL7702 cells (n=3). ${}^{a}P < 0.05$, ${}^{b}P < 0.01$. (F) qRT-PCR analyses of p53, GPX4, SLC7A11, ACSL4 and GSDMD proteins were performed (n = 3 in every group). ${}^{a}P < 0.05$, ${}^{b}P < 0.01$. (G) Western blot analyses of p53, GPX4 and GSDMD proteins were performed (n = 3 in every group). ${}^{b}P < 0.01$.(H) Western blot analyses of SLC7A11 and ACSL4 proteins were performed (n = 3 in every group). ${}^{a}P < 0.05$, ${}^{b}P < 0.01$.

Upregulation of p53 downregulates SLC7A11 and GPX4, leading to ferroptosis and triggering of pyroptosis

To further validate our hypothesis, we used nutlin-3α and RSL3 (ferroptosis inducer, which also causes GPX4 inactivation) [21,22] in ALF model mice. H&E staining of liver tissue showed that the administration of nutlin-3α dramatically aggravated liver injury in ALF model mice to the same extent as that with RSL3 (Figure 4A). Furthermore, both treatments shortened the survival time of mice (Figure 4B). We also found that nutlin-3α and RSL3 worsened the inflammatory response in ALF model mice (Figure 4C). GPX4 and SLC7A11 were significantly decreased after nutlin-3α treatment, and ACSL4 protein levels were elevated (Figure 4D), accompanied by increased iron deposition (Figure 4F). Notably, p53 protein levels were upregulated slightly after RSL3 treatment, but this was not significant (Figure 4D). Western blotting showed that GSDMD and GSDMD-N protein levels were

significantly higher in the nutlin-3α and RSL3 groups than in the ALF model group (Figure 4E). Immunofluorescence staining showed that nutlin-3α and RSL3 significantly exacerbated GSDMD expression in liver tissue, which suggested that inducing ferroptosis aggravated pyroptosis (Figure S1B). Taken together, these data indicate that p53 upregulation may cause SLC7A11 and GPX4 downregulation, leading to ferroptosis, which in turn triggers pyroptosis to amplify the inflammatory response. This process may form a positive feedback loop, resulting in the deterioration of ALF.

FIGURE 4 Activation of the p53/GPX4/GSDMD signaling pathway exacerbated ALF. (A) Macroscopic examinations of mouse livers were collected, and liver sections were stained with H&E(100×). a: normal group general image, b: model group general image, c: p53 inducer group general image, d: ferroptosis inducer group general image, e: normal group microscope image, f: model group microscope image, g: p53 inducer group microscope image, h: ferroptosis inducer group microscope image. (B) The administration of Nutlin-3 α and RSL3 shortened the survival time of mice treated with LPS/ D-GalN. (C) Multi-factor kit for the detection of IL-1 β , TNF- α , IL-6, IL-2 and CCL2 in mouse serum. $^aP < 0.05$, $^bP < 0.01$.(D) Western blot analyses of p53, GPX4, SLC7A11, ACSL4 and GSDMD proteins were performed (n = 3 in every group). $^aP < 0.05$, $^bP < 0.01$.(E) Western blot analyses of GSDMD protein were performed (n = 3 in every group). $^aP < 0.05$, $^bP < 0.01$.(F) Iron Kit for Iron Detection. $^bP < 0.01$.

The SIRT1-mediated p53/GPX4/GSDMD signaling pathway is dependent on p53 deacetylation in LPS/D-GalN-induced ALF

We found that SIRT1 levels were downregulated in human ALF, while Ac-p53 and p53 levels were increased (Figure 1D, E). Previous studies have shown that SIRT1 inhibits p53 deacetylation. Our results confirmed that p53/GPX4/GSDMD mediated ferroptosis and pyroptosis. Therefore, we next pre-treated mice with EX527 and resveratrol. H&E staining showed that the structure of the liver lobules was severely destroyed by the infiltration of inflammatory cells in the EX527 group compared with

the ALF model group. In contrast, resveratrol treatment attenuated LPS/D-GalNinduced acute liver injury (Figure 5A) and prolonged the survival time of mice (Figure 5B). Multi-factor kits showed that EX527 exacerbated the inflammatory response (serum IL-1β, TNF-α, IL-6, IL-2, and CCL2 levels in mice), while resveratrol had the opposite effect (Figure 5C). Western blotting showed that, in liver tissue of resveratrol-treated mice induced with ALF, SIRT1 activation increased p53 acetylation, with no significant changes in p53 protein levels (Figure 5D). When SIRT1 was inhibited, GPX4 and SLC7A11 expression was decreased and ACSL4 expression was upregulated (Figure 5E). GSDMD and N-GSDMD expression was increased, especially GSDMD-N (Figure 6A), and iron accumulation was enhanced (Figure 6B). We further performed immunofluorescence experiments, which showed no significant change in p53 protein expression in the RSV or EX527 treatment groups compared with the ALF model group (Figure 6C), which is consistent with our results mentioned above (Figure 5D). Overall, these data demonstrate that SIRT1 exerts protection against ALF by inhibiting p53 deacetylation, thereby inhibiting the GPX4/GSDMD signaling pathway.

FIGURE 5 SIRT1 interdicts the GPX4/GSDMD signaling pathway by intercepting p53 deacetylation. (A) Macroscopic examinations of mouse livers were collected, and liver sections were stained with H&E (100×). a: normal group general image, b: model group general image, c: SIRT1 inducer group general image, d: SIRT1 inhibitor group general image, e: normal group microscope image, f: model group microscope image, g: SIRT1 inducer group microscope image, h: SIRT1 inhibitor group microscope image. (B) Survival time of mice after RSV and EX527 treatments (C) Multi-factor kit for the detection of IL-1 β , TNF- α , IL-6, IL-2 and CCL2 in mouse serum. ${}^{a}P < 0.05$, ${}^{b}P < 0.01$. (D-E) Western blot analyses of SIRT1, Ac-p53, p53, GPX4, SLC7A11 and ACSL4 proteins were performed (n = 3 in every group). ${}^{a}P < 0.05$, ${}^{b}P < 0.01$.

FIGURE 6 SIRT1 interdicts the GPX4/GSDMD signaling pathway by intercepting

p53 deacetylation. (A) Western blot analyse of GSDMD protein was performed (n = 3 in every group). ${}^{b}P < 0.01$. (B) Iron Kit for Iron Detection. Data were presented as the mean \pm SD of 5 independent experiments. ${}^{a}P < 0.05$, ${}^{b}P < 0.01$. (C-D) SIRT1 and p53 expression in liver tissue were measured by immunofluorescence (100×). a: normal group microscope image, b: model group microscope image, c: SIRT1 inducer group microscope image, d: SIRT1 inhibitor group microscope image. ${}^{a}P < 0.05$, ${}^{b}P < 0.01$.

SIRT1 attenuates hepatocyte ferroptosis and pyroptosis via a p53/GPX4/GSDMD-dependent mechanism

To further investigate the functional role of SIRT1 in hepatocyte ferroptosis and pyroptosis, we knocked down and overexpressed SIRT1 in HL7702 cells. ALT and AST levels were lower in the SIRT1 overexpression group and higher in the SIRT1 knockdown group than in the ALF model and knockdown groups (Figure 7A, B). Ferroptotic events (elevation of ROS activity and iron accumulation) were detected in the SIRT1 overexpression group (Figure 7C, D). Western blotting showed that Ac-P53 protein levels were significantly decreased in the SIRT1 overexpression group, while p53 did not change (Figure 7E). We next examined ferroptosis- and pyroptosis-related proteins (GPX4, SLC7A11, ACSL4, and GSDMD). We found that upregulation of SIRT1 increased GPX4 and SLC7A11 protein expression and decreased ACSL4 and GSDMD protein expression (Figure 7F, G). Furthermore, knockdown of SIRT1 inhibited the deacetylation and degradation of p53 and downregulated levels of SLC7A11 and GPX4 (Figure 7F–G). These data showed that SIRT1 overexpression alleviated ALF in HL7702 cells via a p53/GPX4/GSDMD-dependent mechanism.

FIGURE 7 SIRT1 attenuates hepatocyte ferroptosis and pyroptosis via p53/GPX4 / GSDMD- dependent mechanism in vitro. (A-B) The levels of AST and ALT were changed in serum samples of HL7702 cells (n=3). $^bP < 0.01$. (C-D) The levels of Iron and ROS were changed in serum samples of HL7702 cells (n=3). $^bP < 0.01$. (E) Western blot analyses of SIRT1, p53 and Ac-p53 proteins were performed (n = 3 in every group). $^bP < 0.01$. (F) Western blot analyses of GSDMD and GPX4 proteins were performed (n = 3 in every group). $^bP < 0.01$. (G) Western blot analyses of

SLC7A11 and ACSL4 proteins were performed (n = 3 in every group). ${}^{b}P < 0.01$.

DISCUSSION

ALF is a life-threatening disease with high morbidity and mortality rates. The most effective treatment for ALF at present is liver transplantation [23]. However, liver transplants are not widely available because of the lack of donors and the high cost of medical care [18]. ALF is characterized by extensive hepatocellular cell death, leading to massive loss of parenchymal cells, with the release of cell contents, cell swelling, and inflammation. Emerging evidence has indicated that ferroptosis and pyroptosis, two newly identified forms of non-apoptotic cell death, play a crucial role in liver disease [24, 25], but their precise role in ALF is unknown. In this study, we provided evidence that ferroptosis and pyroptosis occurred in ALF and established an association between them. We found that SIRT1 activation or inhibition of the p53/GPX4/GSDMD signaling pathway attenuated LPS/D-GalN-induced ferroptosis and pyroptosis in ALF (Figure 8).

In this study, we found that the activity of the enzymatic biomarkers ALT and AST was markedly increased in human ALF, accompanied by elevated inflammatory factors, such as TNF-α, IL-1β, and IL-6. Furthermore, we found that the ferroptosis-related antioxidant proteins GPX4 and SLC7A11 were reduced and iron deposition was aggravated. Additionally, GSDMD expression was increased.

The pathogenesis of ALF induced by LPS/D-GalN in mice is similar to that of fulminant hepatitis in humans^[26, 27]. Only some evidence has indicated that ferroptosis and pyroptosis occur in LPS/D-GalN-induced ALF, and inhibition of ferroptosis and pyroptosis attenuates ALF^[28, 29]. However, the association between ferroptosis and pyroptosis is unclear.

GPX4 and GSDMD play a prominent role in the occurrence of ferroptosis and pyroptosis. GSH biosynthesis and proper functioning of GPX4 are critical for inhibiting ferroptosis, and conditions that culminate in GPX4 inhibition/destabilization sensitize cells to ferroptosis or even trigger ferroptotic cell death^{[19, 21], [30]}. GSDMD, a mediator of pyroptosis, is cleaved by inflammasome-

activated caspase-1 and LPS-activated caspase-11/4/5 into active GSDMD-N and inactive GSDMD-C. Deletion of GSDMD completely abolishes cell pyroptosis^[31, 32]. An increasing number of studies have suggested that there is an interaction between ferroptosis and pyroptosis. The knockout of caspase-11, which is involved in the nonclassical pathway of pyroptotic cell death, in myeloid cells conferred similar protection in septic myeloid cell-specific GPX4-knockout mice, which were susceptible to lethal infection^[33]. The caspase-1-dependent NLRP3 inflammasome was also inhibited by GPX4, indicating that GPX4 has a broad role in inhibiting pyroptosis [33]. However, the association between ferroptosis and pyroptosis in ALF is unclear. The present study provided evidence that bridged the gap between ferroptosis and pyroptosis, and showed that blocking the p53/GPX4/GSDMD pathway regulated ferroptosis and pyroptosis in ALF. Inhibiting p53 and enhancing GPX4 in ALF model mice by drugs reduced AST and ALT levels and inflammatory reactions compared with the ALF model group, and ferroptotic events (depletion of GPX4, GSH, and SLC7A11, and iron accumulation) were reversed. Additionally, GSDMD-N protein levels were significantly decreased, consistent with the immunofluorescence results (Figure S1). Notably, deletion of GSDMD decreased p53 expression and upregulated GPX4, which indicated crosstalk between ferroptosis and pyroptosis. The knockdown of GPX4 increased AST and ALT levels, accompanied by significantly increased ferroptotic markers and GSDMD (Figure S2). Together, these results suggested that blocking the p53/GPX4/GSDMD signaling pathway alleviated ferroptosis and pyroptosis in ALF, and a positive feedback loop may exist. In our study, we found that increased or decreased GPX4 mRNA or protein expression did not affect p53, but it acted indirectly by regulating GSDMD, suggesting that GPX4 is a downstream regulator of p53. Chen^[34] et al reported that p53 levels were unaffected by the loss of ACSL4 and GPX4, and p53-driven ferroptosis was induced in a GPX4-independent manner. Nevertheless, enhancement of GPX4 reduced p53 transcription, which was inconsistent with the western blotting results. This difference between mRNA and protein levels suggests that post-transcriptional regulation, translational efficiency, and post-translational modifications alter protein levels. One

possible explanation for this difference is that reduced translational efficiency may be compensated for by increased transcriptional activity^[35]. However, the mechanism underlying the differences in transcription and translation of p53 is unclear. SIRT1 has been widely reported to play a protective role in various biological processes including nutrient starvation, DNA repair, aging, oxidative stress, and the inflammatory response [36, 37]. One study suggested that negative regulation of SIRT1 increased pyroptosis (GSDMD) and aggravated the acute hepatic pro-inflammatory reaction [38]. This finding is consistent with another study, which showed that SIRT1 was suppressed in APAP-induced hepatotoxicity [39]. Treatment with resveratrol, a small-molecule SIRT1 activator, shows a protective function in mouse liver ischemiareperfusion injury [40, 41]. Similarly, in our study, we found that SIRT1 was decreased and p53 and Ac-p53 were increased in human ALF. SIRT1 is an NAD-dependent deacetylase that directly deacetylates p53 and mediates its function^[37]. A study showed that SIRT1 overexpression abolished p53 acetylation levels and reduced the release of hepatic enzymes, hepatic oxidative, stress, and inflammation in nonalcoholic fatty liver disease [42]. Ma[43] et al demonstrated that SIRT1 inhibited ferroptosis-induced myocardial cell death through the p53/SLC7A11 axis in myocardial ischemia-reperfusion injury. Nevertheless, whether SIRT1 activation regulates p53 deacetylation to affect ferroptosis in ALF has not been shown. Our study showed that SIRT1 activation attenuated liver injury and the inflammatory response, accompanied by a reduction in ferroptosis and pyroptosis-related proteins in ALF. We demonstrated that SIRT1 activation inhibited p53/GPX4/GSDMD by inducing p53 acetylation, which attenuated LPS/D-GalN-induced ALF. In conclusion, our study provides evidence that ferroptosis and pyroptosis are crucial modes of hepatocyte death in ALF, and the interactions between these modes of cell death advance the progression of ALF. SIRT1 plays an important role in ALF through p53/GPX4/GSDMD-mediated ferroptosis and pyroptosis. These results could provide a new therapeutic target to alleviate ALF. However, there are still many issues that need to be further investigated. First, p53 is a versatile protein with multiple roles in promoting physiological and pathological regulation. Although p53 can promote

ferroptosis, it is also involved in several major functions, such as cell cycle arrest, DNA repair, angiogenesis, metastasis, and senescence. When p53 pro-death function is inhibited, its pro-survival function is concomitantly impaired. Therefore, how the unique p53-mediated pro-death function might be achieved is unclear. Second, our research was only limited to cellular and mouse models and has not been applied to clinical studies. Although we found decreased SIRT1 expression in human ALF liver tissue, whether an SIRT1 activator is effective for acute liver injury and failure in patients is unknown, and further safety and efficacy studies are required. Third, the mechanism of ALF may be associated with multiple modes of cell death, but our study was limited to ferroptosis and pyroptosis, and was not designed to examine other modes of death. The focus of our next study will be to further investigate the mechanism of acute liver failure in depth.

FIGURE 8 SIRT1 activation ameliorates LPS/ D-GalN-induced acute liver failure by inhibiting p53/GPX4/GSDMD to reduce ferroptosis and pyroptosis. SIRT1 activation inhibit p53 deacetylation and thereby inhibiting the GPX4/GSDMD signaling pathway, reducing inflammatory response and iron deposition. Blocking p53/GPX4/GSDMD signaling pathway attenuates ferroptosis and pyroptosis in ALF

5cknowledgments

We thank Ellen Knapp, PhD, from Liwen Bianji (Edanz) (www.liwenbianji.cn/), for editing the English text of a draft of this manuscript.

ARTICLE HIGHLIGHTS

Research background

ALF has a high mortality with widespread hepatocyte death involving ferroptosis and pyroptosis, but their precise role in ALF is unknown. SIRT1-mediated deacetylation influences multiple biological processes, including cellular senescence, apoptosis, sugar and lipid metabolism, oxidative stress, and inflammation. In this study, we examined the link between ferroptosis and pyroptosis and the upstream regulatory mechanisms.

Research motivation

The most effective treatment for ALF at present is liver transplantation. However, liver transplants are not widely available because of the lack of donors and the high cost of medical care. Therefore, therapies for ALF are imminent.

Research objectives

To explore a link between ferroptosis and pyroptosis and the upstream regulatory mechanisms.

Research methods

Animal and cellular models of ALF were developed. The levels of AST and ALT were tested by Automatic Biochemistry Instrument. Iron, ROS and GSH levels were measured using commercial kits. SIRT1, p53, Ac-p53, GPX4, GSDMD, SLC7A11 and ACSL4 protein expression levels were measured through Western blotting.

Research results

AST and ALT levels were elevated in the serum of ALF patients. SIRT1, SLC7A11, and GPX4 expressions were decreased and Ac-p53, p53, GSDMD, and ACSL4 levels were elevated in human ALF liver tissue. In p53 and ferroptosis inhibitor–treated and GSDMD^{-/-} groups, serum IL-1β, TNF-α, IL-6, IL-2 and CCL2 levels were decreased and hepatic impairment was mitigated. In mice with GSDMD knockout, p53 was reduced, GPX4 was increased, and ferroptotic events (depletion of SLC7A11, elevation of ACSL4, and iron accumulation) were detected.

Research Conclusions

SIRT1 activation attenuated LPS/D-GalN-induced ferroptosis and pyroptosis by inhibiting the p53/GPX4/GSDMD signaling pathway in ALF.

Research perspectives

Our research is only limited to cellular and mouse models and has not been applied to clinical studies. Although we found decreased SIRT1 expression in human ALF liver tissue, whether SIRT1 activator is effective for acute liver injury and failure in patients is unknown, and further safety and efficacy studies are required.

88684.docx

ORIGINALITY REPORT

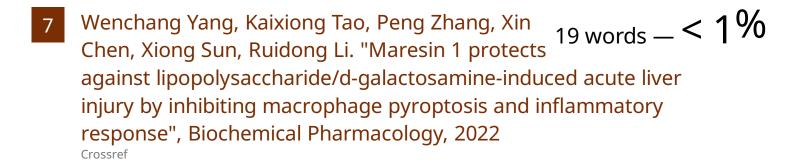
5%

SIMILARITY INDEX

PRIMARY SOURCES

- www.ncbi.nlm.nih.gov
 Internet

 73 words 1 %
- Sha Huang, Yuhua Wang, Shunwen Xie, Yuqi Lai et al. 67 words 1% "Hepatic TGFβr1 Deficiency Attenuates
 Lipopolysaccharide/D-Galactosamine–Induced Acute Liver
 Failure Through Inhibiting GSK3β–Nrf2–Mediated Hepatocyte
 Apoptosis and Ferroptosis", Cellular and Molecular
 Gastroenterology and Hepatology, 2022
- Hui Chen, Xiaoping Lin, Xiaohong Yi, Xiaofeng Liu, Ranghui Yu, Wenhao Fan, Yaping Ling, Yanan Liu, Weidang Xie. "SIRT1-mediated p53 deacetylation inhibits ferroptosis and alleviates heat stress-induced lung epithelial cells injury", International Journal of Hyperthermia, 2022
- $\frac{1}{1}$ sci-hub.se $\frac{1}{1}$ 27 words -<1%
- cardiothoracicsurgery.biomedcentral.com $_{\text{Internet}}$ 24 words -<1%
- 6 www.omicsdi.org
 Internet 21 words < 1%



- Jingbo Wang, Peili Tang, Quan Cai, Sifang Xie, Xueyun Duan, Yuzheng Pan. "Matrine Can Inhibit the Growth of Colorectal Cancer Cells by Inducing Ferroptosis", Natural Product Communications, 2020

 Crossref
- Yangchun Xie, Rui Kang, Daniel J. Klionsky, Daolin Tang. "GPX4 in cell death, autophagy, and disease", Autophagy, 2023

 Crossref
- Yanqing Liu, Wei Gu. "The complexity of p53-mediated metabolic regulation in tumor suppression", Seminars in Cancer Biology, 2021 Crossref
- pubmed.ncbi.nlm.nih.gov

 Internet

 14 words < 1 %
- www.xiahepublishing.com 14 words < 1%
- Kentaro Kadono, Shoichi Kageyama, Kojiro Nakamura, Hirofumi Hirao et al. "Myeloid ikaros– 13 words < 1% SIRT1 signaling axis regulates hepatic inflammation and pyroptosis in ischemia-stressed mouse and human liver", Journal of Hepatology, 2021

EXCLUDE QUOTES ON EXCLUDE SOURCES

EXCLUDE BIBLIOGRAPHY ON EXCLUDE MATCHES

< 12 WORDS

< 12 WORDS